

Extragalactic (Sub)millimeter Astronomy – Today and Tomorrow

Karl M. Menten & Frank Bertoldi

Max-Planck-Institut für Radioastronomie
Auf dem Hügel 69, D-53121 Bonn, Germany
kmenten@mpifr-bonn.mpg.de, bertoldi@mpifr-bonn.mpg.de

Abstract

Recent observations at mid-infrared to millimeter wavelengths have opened up the distant universe to detailed investigations of the star forming properties of galaxies, and the role of active galactic nuclei in the energetics of galaxies. We discuss observations of dust emission at high-redshift, and describe some of the most important new (sub)millimeter instruments to become available within this decade.

1 Introduction

Many important questions of extragalactic astronomy are uniquely addressed by observations in the (sub)millimeter and far-infrared wavelength regime:

- What are the physical conditions in the interstellar medium of various types of galaxies?
- What is the powering source of ultraluminous infrared galaxies?
- What is the star formation history of the universe at early epochs? Is a major part of the early star formation obscured by dust and thus unobservable at optical wavelengths?

In all of these areas, significant progress has been made recently as a result of new instrumental developments, such as the highly successful *Infrared Space Observatory* (ISO) mission, the coming of age of millimeter-wavelength interferometry, allowing (sub)arcsecond imaging of molecular gas, and the availability of sensitive (sub)millimeter bolometer arrays for the detection of weak dust emission even from very high redshift objects.

Here we summarize recent results on the latter subject and then describe some of the most important new (sub)millimeter instruments to become available within this decade. Finally, we describe the impact of these new instruments on important areas of extragalactic astronomy.



Figure 1: *Left:* The *Max-Planck Millimeter Bolometer* “MAMBO”, a 37-element array bolometer sensitive to radiation with wavelengths from 1.0 to 1.4 mm (Kreysa et al. 1999). The opened cryostat reveals the 5 mm diameter feed horns that collimate the incident radiation onto germanium semiconductor elements, which are cooled to 0.3 K. *Right:* The IRAM 30 m telescope on Pico Veleta in the Spanish Sierra Nevada.

2 Star formation in the Early Universe

When did Galaxies first form in the Early Universe, and when did the stars form within them? With the most powerful telescopes we are today able to observe light from galaxies that was emitted over ten billion years ago, at a time when the universe was only a few billion years old. During these “dark ages” the first galaxies formed, and in these the first stars and black holes. The large crowding of mass condensations in the yet small Universe lead to frequent collisions and mergers during which smaller structures grew to larger galaxies. The strong tidal forces in such encounters caused strong perturbations in the interstellar gas of the galaxies, which partly grew to dense agglomerations in which rapid and intense bursts of star formation occurred. It is possible that a large fraction of all stars ever created in the Universe formed in such “starbursts” during galaxy formation.

In order to reconstruct the star formation history of the Universe one needs to obtain representative samples of the galaxy population at all epochs. Such observations must cover spectral ranges which permit an estimate of the instantaneous star formation rate in these objects. Observations with heat-sensitive bolometer array cameras now for the first time permit an unobscured view on starburst galaxies and on active galactic nuclei (AGN or quasars) in the Early Universe.

2.1 The extragalactic infrared background

Deep optical ($0.2 \mu\text{m} - 1 \mu\text{m}$) and near-infrared (NIR: $1 \mu\text{m} - 3 \mu\text{m}$) observations with the Hubble Space Telescope show a sky covered densely with very distant galaxies (Lilly et al. 1996; Madau et al. 1996). If we had an unobscured view on their star-forming regions, then the (rest frame) ultraviolet radiation

emitted by the short-lived most massive stars in such regions would provide a good measure of the instantaneous star formation rate. However, the regions most proficiently forming stars tend to be deeply embedded in dusty molecular clouds, which preferentially absorb the short wavelength UV and optical radiation. Many of the intrinsically brightest star-forming regions therefore remain optically obscured.

Deep mid-infrared (MIR: $5\ \mu\text{m} - 15\ \mu\text{m}$) imaging with the *Infrared Space Observatory* (ISO, Aussel et al. 1999), as well as millimeter and sub-millimeter ($850\ \mu\text{m} - 1200\ \mu\text{m}$) imaging with the SCUBA Bolometer camera at the *James Clerk Maxwell Telescope* (JCMT; e.g. Smail et al. 1997, Eales et al. 1999) and with the *Max-Planck Millimeter Bolometer* (“MAMBO”: Fig. 1) at the IRAM 30 m telescope in southern Spain (Bertoldi et al. 2000) yield a picture which is significantly different from what we learned from optical images. Far fewer objects dominate the MIR background, which arises from warm dust in distant galaxies. The far-infrared (FIR: $30\ \mu\text{m} - 300\ \mu\text{m}$) background radiation, which best traces the heated dust, was initially found from a low-resolution sky survey with the *Cosmic Background Explorer* satellite (COBE, Puget et al. 1996). With SCUBA and MAMBO, this unresolved FIR background was later resolved into individual objects, which are now being identified with high-redshift, optically faint galaxies (Hughes et al. 1998).

If the FIR/mm background indeed arises from star-forming regions in the Early Universe, the energy flux of this radiation would be so large that it could account for the formation of a large fraction of all stars ever formed in the Universe. The FIR/mm background radiation would then be the ideal tracer of the star formation history of the Universe.

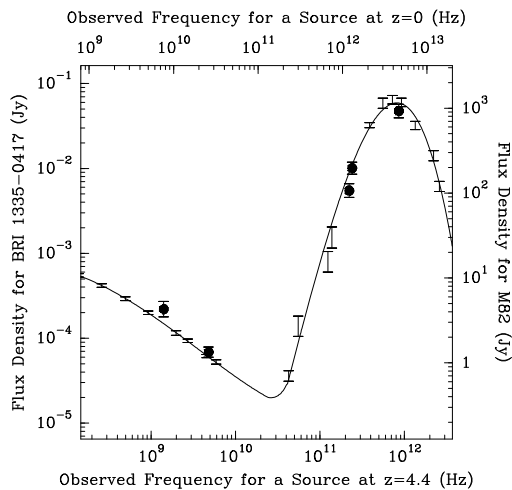


Figure 2: Spectral energy distribution of the typical, nearby starburst galaxy M82 (error bars). At low frequencies, the synchrotron emission from supernovae produces a shallow decline of flux density with frequency, whereas at mm to IR wavelengths, the thermal emission of dust shows a greybody spectrum with a steep rise at sub-mm wavelengths. Also shown (dots) are flux densities measured for the $z = 4.4$ quasar 1335-0417 (Carilli et al. 1999a).

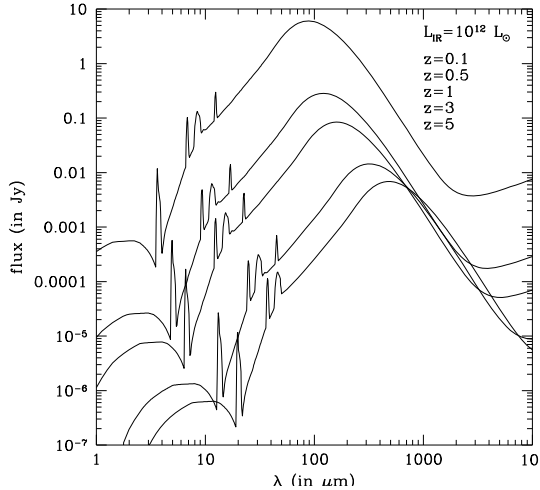


Figure 3: A typical starburst SED viewed at increasing redshift. At sub-mm and mm wavelengths, the flux density remains nearly constant at redshifts from 0.5 to over 5. (from Guiderdoni et al. 2000)

2.2 Distance

Today, intensive efforts aim at discovering a sufficient number of the FIR/mm background sources, and to determine their spectral properties and redshifts. Up to now, only a few dozen sources have been found, and for only four sources accurate spectroscopic redshift were determined. For another eighteen sources, the redshift, z , can be estimated from the ratio between the mm and radio ($\lambda = 20$ cm) flux densities (Carilli et al. 1999b; Carilli & Yun 1999, 2000; Dunne et al. 2000).

Such estimates take advantage of the fact that typical star-forming galaxies have a radio-to-FIR spectral energy distribution (SED, Fig. 2) which at radio wavelengths shows a shallow decline in flux density, $F_\nu \propto \nu^{-0.7}$, but at frequencies $\nu > 100$ GHz, a steep rise, $F_\nu \propto \nu^{3.5}$. The flux ratio $F_\nu(350 \text{ GHz})/F_\nu(1.4 \text{ GHz})$ therefore increases significantly with increasing redshift, and z can be estimated from the observed flux ratio. Although the resulting redshift estimates are affected by a large scatter of actual galaxy SEDs around the assumed “typical” SED, the resulting redshifts permit a first glance at the redshift distribution of those FIR/mm background objects for which radio fluxes or upper limits thereof were measured (Fig. 4).

The steep rise in flux density with decreasing wavelength at mm and sub-mm wavelengths leads for a given source luminosity to an observed flux density (at fixed wavelength) which is nearly independent of redshift for z between 0.5 and > 5 (Fig. 3). At mm and sub-mm wavelengths this “negative K-correction” permits a complete census of all high-redshift objects which are brighter than the given observational detection limit.

Under the assumption that star formation – and not accreting black holes in AGN – dominate the emission of the FIR/mm background sources, the deduced redshift distribution (Fig. 4) shows that the majority of all FIR/mm sources are at $z \approx 2$ to 4. A large fraction of all stars in the universe thus

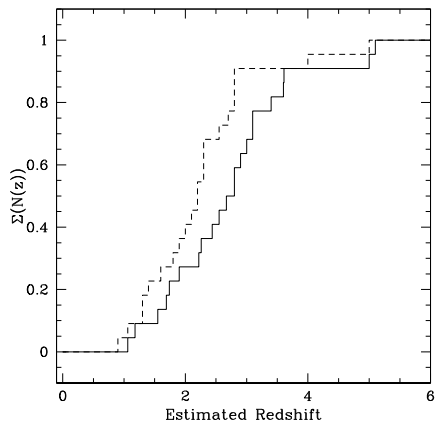


Figure 4: Cumulative redshift distribution (fraction of sources at smaller than a given redshift) of 22 FIR/mm sources. For 4 sources, redshifts were determined spectroscopically, for 18 they are based on the radio (20 cm) to 850 μm or 1.2 mm flux ratio. The two curves are based on different calibrations through nearby galaxy SEDs.

appears to have formed within the first 4 billion years after the Big Bang. Moreover, these stars formed in bursts of very high star formation rates, typically about one thousand solar masses per year. To sustain such star formation rates for at least a dynamical time, the objects must have been very massive, comparable to the most massive galaxies seen today: large ellipticals. The redshift distribution of the bright, massive objects may yield clues about the structure formation process in the Early Universe. Amazingly, the estimated redshift distribution shown in Fig. 4 agrees very well with the predictions of a simple analytical model for the collapse of 10^{12} solar mass objects in a cold dark matter dominated universe. Large area surveys for (sub)mm background sources will be able also to investigate their clustering properties, which may yield important constraints on the semi-analytic models of star formation in newly formed galaxies.

2.3 Brightness distribution

Figure 5 shows the brightness distribution of the known FIR/mm background sources. To obtain good statistics also for the brighter objects, sufficiently large, unbiased regions in the sky must be surveyed. The first such “blank field surveys” were conducted with SCUBA at 850 μm . In a total observed area of about 100 square arcminutes several dozen objects were discovered (see Barger et al. 1999). Many of the SCUBA surveys targeted galaxy clusters to take advantage of the brightening of the distant sub-mm sources by gravitational lensing from the foreground cluster (Smail et al. 1997). Galaxy clusters are like magnifying glasses which permit a deeper look at the faint FIR/mm background population. For the source statistics however, lens-amplified sources are problematic because the amplification factor, which is of order 2 or 3, cannot be determined for individual objects.

The SCUBA deep surveys showed that the brightness distribution of the FIR/mm background sources drops steadily up to 850 μm flux densities of

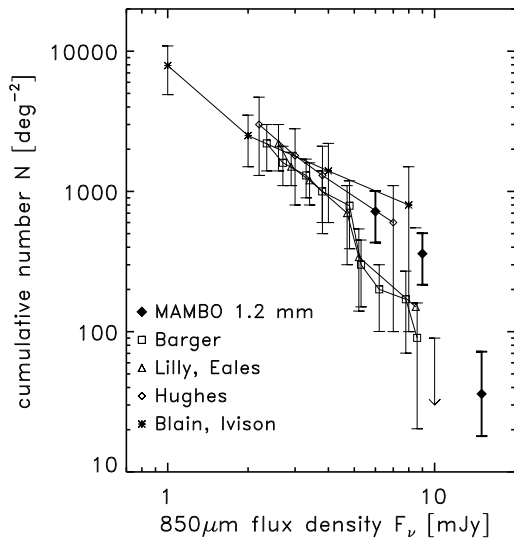


Figure 5: The cumulative brightness distribution (number of objects per square degree brighter than a given $850 \mu\text{m}$ flux density) of sources found in SCUBA and MAMBO deep imaging surveys. MAMBO 1.2 mm fluxes were multiplied by three for comparison with SCUBA $850 \mu\text{m}$ fluxes, assuming a typical sub-mm greybody SED $F_\nu \propto \nu^{3.5}$.

about 5 mJy (1 milli-Jansky = $10^{-29} \text{ W m}^{-2} \text{ Hertz}^{-1}$), but at higher fluxes there appears to be a steep drop in the source counts (Fig. 5). However, the area yet covered with SCUBA observations is too small to provide reliable source count statistics above 5 mJy. Recent MAMBO observations at 1.2 mm in fact show that the turnover cannot be as dramatic as SCUBA observations had indicated.

2.4 Starbursts or quasars?

The brightest background sources provide important clues about the history of structure and star formation in the Early Universe. Galaxies at redshifts between 2 and 4 with $850 \mu\text{m}$ flux densities of 10 to 20 mJy (corresponding to 3 to 6 mJy at 1.2 mm) have total infrared luminosities of order 10^{13} solar luminosities, which implies star formation rates of order $1000 M_\odot \text{ yr}^{-1}$, provided all the energy arises from young stars. Such star formation rates are about ten times higher than those found in the brightest nearby starburst galaxies. They are also ten times higher than those which are derived from the blue luminosities of optically selected high-redshift galaxies. The unusually bright FIR/mm sources probably reflect some very special conditions during star- and galaxy formation in the Early Universe.

However, due to the small number of known FIR/mm background sources it remains unclear whether these sources are indeed strong starburst galaxies, whether they are merely lens-amplified normal star-forming galaxies, or if they could be quasars in which an accreting black hole provides the vast energies

which are partially reemitted by the circumnuclear dust. Determinations of the surface density and of the spectral and morphological properties of the brightest FIR/mm sources are important, yet missing pieces for a better understanding of the star and galaxy formation history of the Universe.

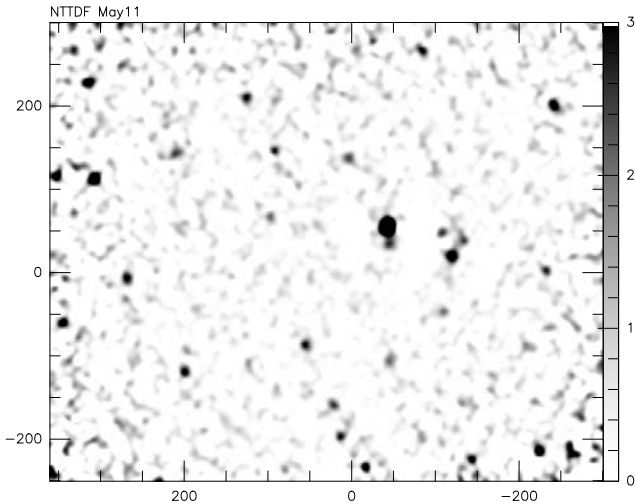


Figure 6: MAMBO 1.2 mm map around the 15 mJy bright $z = 4.7$ quasar BR1202-0725. Units are mJy and arcseconds. The RMS noise level rises from ~ 0.4 mJy at the image center to ~ 0.8 mJy near the edges. Over one dozen bright mm background sources are visible.

2.5 Deep MAMBO surveys

Observations with MAMBO at the IRAM 30 m telescope aim at a better determination of the surface density and the properties of the brightest mm background sources. During the last two winter observing campaigns we mapped three fields with a total area of ~ 300 arcmin² to a detection limit of ~ 2 mJy, which corresponds to 6 mJy at $850 \mu\text{m}$. A preliminary data analysis reveals at least a dozen sources alone in the fields surrounding the $z = 4.7$ quasar BR1202-0725 (Fig. 6), with two sources even brighter than 5 mJy. These observations for the first time show that background sources brighter than 5 mJy at 1.2 mm are sufficiently abundant that significant counts can be obtained from fields sizes of order 100 arcmin² (Fig. 5).

2.6 The history of star formation

Adopting a typical dust temperature (30 to 50 K) and initial stellar mass distribution, a given source's mm flux density allows an estimate of its total

luminosity and thus of the star formation rate which would give rise to this luminosity. The observed number and brightness distribution of sources within a given redshift interval then yields a spatially averaged star formation rate at this epoch. Plotting this against redshift shows the star formation history of the universe (Fig. 7).

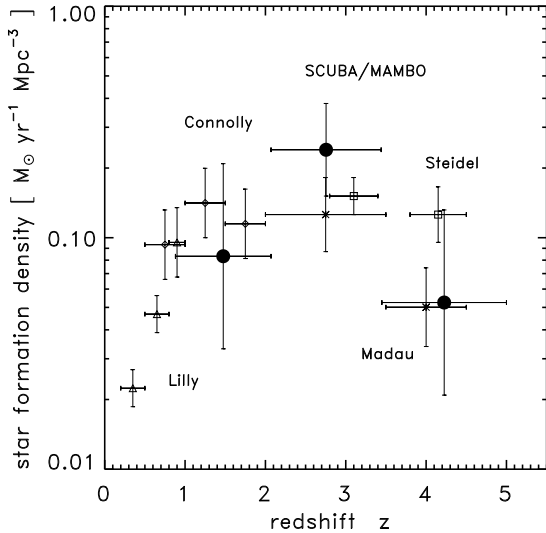


Figure 7: The history of star formation in the universe: the spatially averaged star formation rate is plotted as a function of redshift. Except for the SCUBA/MAMBO points, all data derive from optical observations, corrected for extinction by ≈ 5 .

Initial attempts to determine the spatially averaged star formation rate at high (> 1) redshifts were based on estimates using the galaxies' (rest frame) blue magnitudes (Lilly et al. 1996; Madau et al. 1996). Deep ground-based redshift surveys and an analysis of the Hubble Deep Field galaxies indicated a maximum in the spatially averaged star formation rate at redshift ≈ 1.5 . SCUBA sub-mm surveys now show that the infrared-brightest galaxies are missed by optical surveys. The star formation history derived from SCUBA and MAMBO surveys shows that the star formation rate keeps rising to $z > 3$. Only when the optically-based estimates are corrected for extinction, which cannot be done for individual objects though, then the mm and optical measurements are in rough agreement. Although under debate, it appears that the sub-mm and mm surveys more reliably trace the star formation history of the Universe than optical surveys do. Much progress should be made in the coming years as follow-up observations will better characterize the nature of the (sub)mm background sources, and when larger bolometer arrays (e.g. the upcoming 117-element MAMBO) will allow to survey larger areas.

3 New observatories

All ground-based submillimeter observations are seriously hampered by absorption by and emission from the Earth's atmosphere, which allows effective observations only in a few atmospheric windows. Consequently, major efforts have been and will be made to minimize or, in the case of satellite platforms, overcome this obstacle. Two such platforms, the *Stratospheric Observatory for Infrared Astronomy* (SOFIA) and the *Far Infra-Red and Submillimetre Telescope* (FIRST) satellite mission, will be briefly summarized in the following. Both will carry instrumentation for observations in the (far)infrared and submillimeter regimes.

The diffraction-limited spatial resolution of SOFIA and FIRST at the shortest submillimeter wavelengths ($300\ \mu\text{m}$) will be $\approx 20''$. While this is sufficient for survey observations and studies of the general interstellar medium in nearby galaxies, significantly higher resolution is provided for detailed studies, e.g., of circumnuclear regions and objects at high redshift. This will be provided by the *Atacama Large Millimeter Array* (ALMA), the next generation (sub)millimeter interferometer.

Two other satellite missions, the *Microwave Anisotropy Probe* (MAP)¹ and Planck², to be launched in 2001 and 2007, respectively, will map the Cosmic Microwave Background in various centimeter and (sub)millimeter wavelength bands with unprecedented sensitivities in order to study cosmic structure formation and provide accurate determinations of the cosmological parameters.



Figure 8: The Boeing 747-SP aircraft which is to be modified to contain a 2.5 m telescope, the *Stratospheric Observatory for Infrared Astronomy*.

¹<http://map.gsfc.nasa.gov/>

²http://astro.estec.esa.nl/astrogen/planck/mission_top.html

3.1 SOFIA – the Stratospheric Observatory for Infrared Astronomy

SOFIA³ consists of a 2.5 m telescope installed on a Boeing 747-SP aircraft (see Erickson & Davidson 1995). At its operating altitude of ≈ 13 km the atmospheric absorption is significantly reduced compared to the ground, allowing observations throughout most of the submillimeter and infrared range. While less sensitive than a satellite observatory such as FIRST, throughout its projected twenty year lifetime SOFIA offers the flexibility to employ the best state-of-the-art instrumentation. A collaboration of NASA and the German space agency DLR, SOFIA is expected to begin operations in 2003. It is expected to have a major impact on extragalactic astronomy, allowing high-sensitivity observations with an extremely diverse and ever up-to-date complement of instruments.

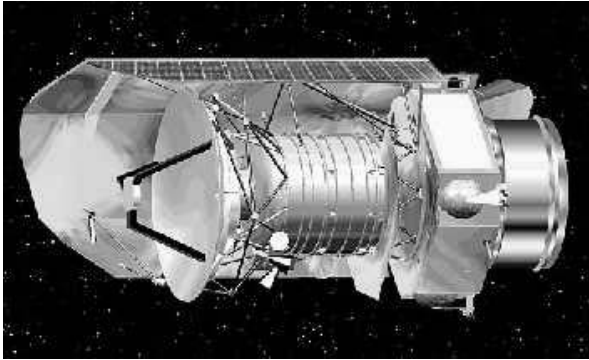


Figure 9: The *Far Infra-Red and Submillimeter Telescope* will perform photometry and spectroscopy in the 60–670 μm range.

3.2 FIRST – the Far Infra-Red and Submillimetre Telescope

The FIRST satellite⁴ (see, e.g., Pilbratt 1998) will be launched by the European Space Agency (ESA) in 2007 to an orbit around the L2 Lagrangian point in the Sun/Earth system. The satellite, which is a collaboration of ESA and NASA, will carry a low emissivity, passively cooled 3.5 m telescope and three science instruments:

- HIFI, the Heterodyne Instrument for FIRST, will perform high resolution spectroscopy in three wide bands between 480 and 2700 GHz covering a vast number of molecular lines and important fine structure lines from atomic and ionic species such as CI, CII, and NII;

³<http://sofia.arc.nasa.gov/> and <http://remotesensing.dlr.de/IR/SOFIA/>

⁴<http://astro.estec.esa.nl/SA-general/Projects/First/first.html>

- PACS, the Photoconductor Array Camera and Spectrometer, comprises two Ge:Ga photoconductor arrays for broadband imaging photometry or medium resolution spectroscopy covering simultaneously the 80–130 and 130–210 μm ranges;
- SPIRE, the Spectral and Photometric Imaging Receiver, will allow broadband imaging photometry in three bands centered at 250, 350, and 500 μm . Each of its bolometer arrays will cover the same $4' \times 4'$ field of view. SPIRE will also allow low resolution spectroscopy covering a smaller $2' \times 2'$ field of view.

In the absence of atmospheric absorption, FIRST has access to the full spectral range covered by its instruments. Among its most important science goals are detailed studies of dust and line emission probing star formation in the early and the local universe. In particular, FIRST will be able to study the main cooling lines of the interstellar medium in the Milky Way and external galaxies with unprecedented sensitivity.

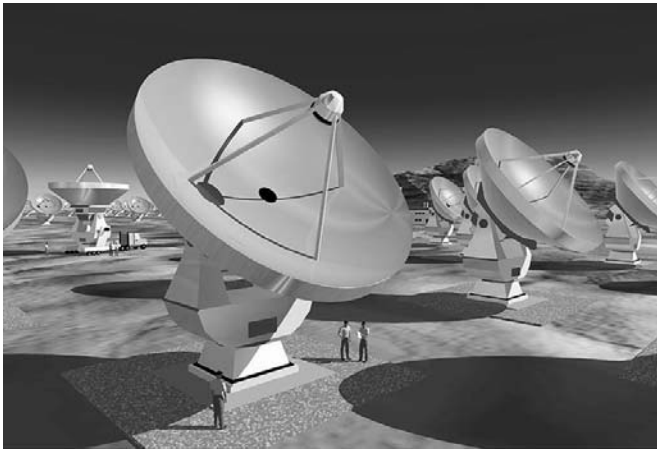


Figure 10: Artist's impression of ALMA.

3.3 ALMA – the Atacama Large Millimeter Array

The *Atacama Large Millimeter Array* (ALMA)⁵ will be comprised of some 64 12-meter sub-millimetre quality antennas, with baselines extending up to 10 km. It will be located on the high-altitude (5000 m) Zona de Chajnantor, east of the village of San Pedro de Atacama in Chile. This is an exceptional site for (sub)millimetre astronomy, possibly unique in the world.

ALMA will revolutionize the field of (sub)millimeter astronomy by opening new vistas in wavelength coverage, spatial resolution, sensitivity, and mapping fidelity.

⁵<http://www.eso.org/projects/alma/> and <http://www.alma.nrao.edu/>

Submillimeter operation is precluded for existing arrays by the relatively low altitudes at which they reside, resulting in significant atmospheric absorption and poor phase coherence, and/or the limited surface accuracy of the telescope dishes. ALMA's excellent site allows efficient submillimeter operation in all the atmospheric windows below 1 THz, with unprecedented sensitivity and a spatial resolution similar to the diffraction limit of large optical/infrared telescopes. Its receivers will cover the range from 70 to 900 GHz.

ALMA's large collecting area, wide bandwidth, and the combination of advanced receiver technology and superior site result in a continuum sensitivity that is ≈ 100 times higher than that of existing instruments.

ALMA is the largest ground-based astronomy project of this decade after VLT/VLTI, and, together with the *Next Generation Space Telescope* (NGST), one of the two major new facilities for world astronomy coming into operation by the end of the this decade.

With ALMA it will be possible to detect and study the earliest and most distant galaxies, the epoch of the first light in the Universe. ALMA will also look deep into the dust-obscured regions where stars are born to examine the details of star and planet formation. In addition to these two main science drivers the array will make major contributions to virtually all fields of astronomical research.

ALMA is a joint merger of the major millimeter array projects into one global project: the *European Large Southern Array* (LSA), the U.S. *Millimeter Array* (MMA), and possibly the Japanese *Large Millimeter and Submillimeter Array* (LMSA).

4 Some important questions

In the following, we list important areas of extragalactic research that will gain particularly much from the new instruments becoming available in the present decade.

Active and normal galaxies in the local universe:

- **Physics and chemistry of the interstellar medium:**

Observations of ionic, atomic, and molecular gas provide important information on the energetics of the interstellar medium of galaxies and its energy sources. For example, ISO measurements of fine structure line emission from species at different ionization levels have addressed the important question whether ultraluminous infrared galaxies are powered by AGN or starbursts (Genzel et al. 1998; Lutz et al. 1998).

The increased sensitivity of SOFIA and FIRST will lead to a dramatic increase in sources that can be studied in fine structure lines. ALMA will complement these observations with high-resolution studies of lines from numerous molecules and neutral carbon and allow imaging of various of the major cooling lines (CII, NII) from intermediate- and high-redshift systems.

- **Where are the molecular circumnuclear tori around AGN?**
The circum-nuclear molecular torus is part of the AGN paradigm (Krolik & Lepp 1989). Extensive searches for absorption of line emission from such a structure against the AGN continuum appear to have found evidence for circumnuclear neutral hydrogen (Conway & Blanco 1995), but clear-cut evidence for molecular absorption from the tori is still elusive (e.g. Drinkwater, Combes & Wiklind 1996). Unusual excitation conditions in the vicinity of the AGN may be responsible for the failure to detect CO in its lower rotational transitions (Maloney et al. 1994).

Current millimeter interferometry allows imaging of molecular *emission* from the central regions of nearby AGN with linear resolutions of order 50 pc, revealing complex kinematics on these size scales (Schinnerer, Eckart & Tacconi 1999). So far, the only direct evidence for circumnuclear molecular material on (sub)parsec scales comes from *Very Long Baseline Interferometry* observations of water maser emission, whose kinematics have been used to determine the mass of the supermassive black hole in NGC 4258 (Miyoshi et al. 1995), as well as its distance (Herrnstein et al. 1999).

ALMA, with its superb sensitivity, angular resolution, and observing bandwidth and its access to higher excitation rotational lines of CO and other molecules, will almost certainly detect circumnuclear gas in the immediate neighborhood of the central engines and provide (sub)parsec resolution imaging for nearby active galaxies.

The high-redshift universe:

- **Clustering:**
If (sub)mm observations of the faint background populations trace the formation of (giant elliptical?) galaxies, then source clustering is expected on mega-parsec scales, corresponding to angular scales of order $1' - 10'$. Larger and deeper imaging surveys will be necessary to establish the clustering properties of the (sub)mm background sources. This should be possible with the next generation bolometer arrays, and eventually with ALMA and FIRST.
- **The high-luminosity end of the source brightness distribution:**
Are the brightest (sub)mm sources powered by starbursts or by AGN? If powered by starbursts, what gives rise to the turnover in their abundance at high luminosities: the mass supply of the host galaxy, limited mass infall rates, or feedback?
- **Redshift determinations:**
Most of the (sub)mm background sources are very faint at optical and near-IR wavelengths, which necessitates large telescopes (Keck, VLT, Gemini, NGST) for follow-up spectroscopy to determine their nature (morphology, optical line ratios and widths) and redshifts. Blind searches

for CO emission may be an efficient alternative once broad-band receivers become available on large single dish (Green Bank Telescope) or interferometer (ALMA) radio and (sub)mm observatories.

- **Onset of AGN activity:**

A large fraction of all high-redshift QSOs show detectable dust emission. What is the energy source for this emission: AGN or starbursts? In general, what is the relation between AGN and starbursts? Do merger events lead to the formation of massive black holes, and when does this occur? Deep optical and infrared studies (VLT, NGST) of the high-redshift AGN, and radio observations with the *Expanded VLA* and with the *Square Kilometer Array* (SKA) should be able to reveal the origin of the thermal emission in high-redshift quasars.

References

- Aussel, H., Cesarsky, C.J., Elbaz, D., Starck, J.L. 1999, A&A 342, 313
- Barger, A.J., Cowie, L.L., Sanders, D.B. 1999, ApJ 518, L5
- Bertoldi, F., Carilli, C., Menten, K.M. et al. 2000, A&A in press
- Carilli, C. L., Menten, K.M., Yun, M.S. 1999a, ApJ 521, L25
- Carilli, C. L., Menten, K.M., Yun, M.S., Bertoldi, F., Owen, F., Dey, A. 1999b, in *Radio Studies of High Redshift Star Forming Galaxies*, astro-ph/9907436
- Carilli, C.L., Yun, M.S. 1999, ApJ 513, L13
- Carilli, C.L., Yun, M.S. 2000, ApJ 530, 816
- Conway, J.E., Blanco, P.R. 1995, ApJ 449, L131
- Dunne, L., Clements, D., Eales, S. 2000, MNRAS, in press (astro-ph 0002436)
- Drinkwater, M.J., Combes, F., Wiklind, T. 1996, A&A 312, 771
- Eales, S., Lilly, S., Gear, W., et al. 1999, ApJ 515, 518
- Erickson, E.F., Davidson, J.A. 1995, in the Proceedings of the Airborne Astronomy Symposium on the Galactic Ecosystem: From Gas to Stars to Dust, eds. M. R. Haas, J. A. Davidson, & E. F. Erickson (San Francisco: ASP), 707
- Genzel, R. et al. 1998, ApJ 498, 579
- Guiderdoni, B., Hivon, E., Bouchet, F.R., Maffei, B. 2000, MNRAS, in print
- Herrnstein, J.R., Moran, J.M., Greenhill, L.J., et al. 1999, Nature, 539
- Hughes, D., Serjeant, S., Dunlop, J., et al. 1998, Nature 394, 241
- Kreysa, E., et al. 1999, SPIE 3357, 319
- Krolik, J. H., Lepp, S. 1989, ApJ 347, 179
- Lilly, S.J., Le Fèvre, O., Hammer, F., Crampton, D. 1996, ApJ 460, L1
- Lutz, D., Spoon, H.W., Rigopoulou, D., Moorwood, A.F.M., Genzel, R. 1998, ApJ 505, L103
- Madau, P., Ferguson, H.C., Dickinson, M.E., et al. 1996, MNRAS 283, 1388

- Maloney, P.R., Begelman, M.C., Rees, M.J. 1994, ApJ 432, 606
- Miyoshi, M., Moran, J., Herrnstein, J. et al. 1995, Nature 373, 127
- Pilbratt, G.L. 1998, in Proc. SPIE, 3356, Space Telescopes and Instruments V, eds.
P.Y. Bely & J.B. Breckinridge, 452
- Puget, J.L. et al. 1996, A&A 308, L5
- Schinnerer, E., Eckart, A., Tacconi, L. J. 1999, ApJ 524, L5
- Smail, I., Ivison, R.J., Blain, A.W. 1997, ApJ 490, L5

